

Supplementary Information for

**Preformed Chromatin Topology Assists Transcriptional
Robustness of *Shh* during Limb Development**

Christina Paliou, Philine Guckelberger, Robert Schöpflin, Verena Heinrich, Andrea Esposito, Andrea M. Chiariello, Simona Bianco, Carlo Annunziatella, Johannes Helmuth, Stefan Haas, Ivana Jerković, Norbert Brieske, Lars Wittler, Bernd Timmermann, Mario Nicodemi, Martin Vingron, Stefan Mundlos* and Guillaume Andrey*

*Corresponding authors: Stefan Mundlos, Guillaume Andrey
Email: mundlos@molgen.mpg.de, guillaume.andrey@unige.ch

This PDF file includes:

Supplementary Methods
Figs. S1 to S5
Tables S1 to S2
Captions for movies S1 to S2
References for SI reference citations

Other supplementary materials for this manuscript include the following:

Movies S1 to S2

Supplementary Methods

CRISPR/Cas9 Engineered Allelic Series

Single guide RNAs (sgRNAs) were designed using the CRISPR Design Tool by the Zhang lab (<http://www.genome-engineering.org/crispr/>) (See SI Appendix, Table S2). The Benchling website was used as an alternative tool (<https://benchling.com/>). The selected oligonucleotides had a quality score over 80% and exonic off-target regions less than two. The sgRNAs were synthesized and cloned into the pSpCas9(BB)-2A-Puro (PX459) vector (Addgene) according to the standard protocol (1). The ESCs transfection with the CRISPR guides and the culture were performed as follows: Day 1) MEF CD1 feeder cells seeded onto a gelatin-coated 6-well plate. Day 2) 3×10^5 G4 ES cells were seeded for each transfection. Day 3) Two hours prior to transfection, the ESC medium without Pen/Strep was added. For transfection, a DNA mix consisting of 8 μ g of each pX459-sgRNA vector was combined with 125 μ l OptiMEM, and a transfection mix consisting of 25 μ l FuGene HD (Promega) and 100 μ l OptiMEM (Gibco), were combined and incubated at RT for 15 minutes before being added drop-wise onto the cells. Day 4) Three 6 cm dishes of DR4-puromycin resistant feeders were seeded for each transfection. Day 5) Targeted G4 cells were split onto three DR4 6 cm dishes and a 48-hour selection was initiated by adding puromycin to the ESC medium (final concentration 2 μ g/ml). Day 7) Selection was quenched and recovery initiated by using standard ESC medium. The recovery period was of ca. 4 days. Day 11) Individual clones (ca. 100 for CTCF motif deletions and ca. 200 for the bigger deletions) were picked from the plate and transferred into 96-well plates with CD1 feeders. After 3 days of culture, plates were split in triplicates, two for freezing and one for growth and DNA harvesting. Genotyping was performed by PCR, qPCR analyses (See SI Appendix, Table S1), subcloning into pTA-GFP vector to detect the mutations in both alleles and Sanger sequencing.

ES and feeder cells were tested for mycoplasma contamination using Mycoalert detection kit (Lonza) and Mycoalert assay control set (Lonza).

Whole-mount in situ hybridization (WISH)

The *Shh* mRNA expression in 34-5 somite stage mouse embryos (E10.5) was assessed by whole mount in situ hybridisation (WISH) using a digoxigenin-labeled *Shh* antisense riboprobe transcribed from a cloned *Shh* probe (PCR DIG Probe Synthesis Kit, Roche). All buffers and solutions were treated with DEPC to inactivate RNase enzymes. Embryos were dissected in 1x PBS and fixed in 4 % PFA/ PBS at 4°C overnight. Fixed embryos were washed twice with PBST and dehydrated in increasing serial Methanol dilutions in PBST (25 %, 50 %, 75 % Methanol/ PBST, 2x 100 % Methanol, 10 min in each dilution) and stored at -20°C. The WISH protocol was as follows: Day 1) Embryos were rehydrated in 75 %, 50 % and 25 % Methanol/ PBST, washed twice with PBST (each step for 10 min), bleached in 6 % hydrogen peroxide/ PBST for 1 hour on ice and washed in PBST. E10.5 embryos were treated with 20 μ g/ml Proteinase K for 2 min, washed with 2x with PBST/ glycine to stop the reaction, washed 5x with PBST and fixed for 20 min in 4 % PFA/ 0.2 % glutaraldehyde in PBS/ 0.1 % Tween 20 at RT. After further washing steps with PBST, embryos were incubated at 68°C in L1 buffer (50% deionised formamide, 5x SSC, 1% SDS, 0.1% Tween 20 in DEPC; pH 4.5) for 10 minutes and then, for 1-2 h in H1 buffer (L1 with 0.1% tRNA and 0.05% heparin). The DIG probes, prior use, were diluted in H1 buffer and denatured for 10 min in 80°C. Afterwards, embryos were incubated ON at 68°C in hybridisation buffer 2 (hybridisation buffer 1 with 0.1% tRNA and 0.05% heparin and 1:100 DIG-*Shh* probe). Day 2) All buffers (L1, L2, L3) were heated to 68°C. The embryos were washed

sequentially 3x 30 min in L1, 3x 30 min in L2 (50% deionised formamide, 2x SSC pH 4.5, 0.1% Tween 20 in DEPC; pH 4.5) and 1x 15 min in L3 (2x SSC pH 4.5, 0.1% Tween 20 in DEPC; pH 4.5) at 68°C to remove the unbound probe. After cooling down to room temperature, the embryos were washed in 1:1 L3 buffer/ RNase solution (0.1 M NaCl, 0.01 M Tris pH 7.5, 0.2% Tween 20, 100 µg/ml RNase A in H₂O) for 5 min. They were then treated for 2x 30 min in RNase solution containing 100 µg/ml RNaseA at 37°C and washed with 1:1 RNase solution/TBST-1 (140mM NaCl, 2.7mM KCl, 25mM Tris-HCl, 1% Tween 20; pH 7.5) for 5 min. After 3x 5 min washing in TBST-1 at RT, the embryos were incubated in blocking solution (TBST 1 with 2% calf-serum and 0.2% BSA) for 2h shaking at RT. The antibody anti-Digoxigenin-AP (Roche, # 11093274910) was also diluted in blocking solution (1:5000) and incubated for 1h rotating at 4°C. Finally, antibody solution was added to the embryos and ON incubation on a shaker followed. Day 3) Removal of unbound antibody was done through a series of washing steps 8x 30 min at RT with TBST 2 (TBST with 0.1% Tween 20, and 0.05% levamisole/tetramisole) and left ON at 4°C. Day 4) Embryos were washed 3x 20 min in alkaline phosphatase buffer (0.02 M NaCl, 0.05 M MgCl₂, 0.1% Tween 20, 0.1 M Tris-HCl, and 0.05% levamisole/tetramisole in H₂O) and antibody detection was carried out in BM Purple AP-substrate (Roche) until a clear signal appeared. Embryos were then washed twice in alkaline phosphatase buffer, fixed in 4 % PFA/ PBS/ 0,2 % glutaraldehyde and 5mM EDTA and stored at 4°C. Limb buds from at least two embryos were analysed from each mutant genotype. The stained limb buds were imaged using Zeiss Discovery V.12 microscope and Leica DFC420 digital camera.

Skeletal Preparation

Foetuses were kept in H₂O for 1-2 hours at RT and heat shocked at 65°C for 1 minute. The skin and the abdominal and thoracic viscera were removed using forceps. The embryos were then fixed ON in 100% technical EtOH in RT. To stain the cartilage of the embryos blue, EtOH was replaced by Alcian Blue (150 mg/ l Alcian Blue 8GX (Sigma-Aldrich) and stained ON in RT. Upon second fixation of the embryos in 100% technical EtOH ON, they were treated with 1% KOH for 15 min for some partial tissue digestion. Then, the membranous bone was stained red using Alizarin Red solution (50 mg/l Alizarin Red (Sigma-Aldrich) in 0.2 % KOH/ bid H₂O). Staining was performed for up to 2 days with visual inspection of each specimen for proper red staining. Remaining tissue was gradually digested in 0.2% KOH-25% glycerol solution. Digestion was completely stopped by placing preparations in 25% glycerol for further clearing and 30% glycerol for short-term storage. Documentation of the skeletal preparations was done in either 25% or 30% glycerol. For long-term storage, 60% glycerol was used. The stained embryos were imaged using Zeiss Discovery V.12 microscope and Leica DFC420 digital camera.

ATAC-seq

Tissues were homogenized using the Ultra Turrax T8 disperser (IKA). 5x10⁴ cells were used per biological replicate. The cells were washed in cold D-PBS (Gibco™ #14190169) and lysed in fresh lysis buffer (10mM TrisCl pH7.4, 10mM NaCl, 3mM MgCl₂, 0.1% (v/v) Igepal CA-630) for 10 min while being centrifuged. Then, supernatant was discarded and cells were prepared for the transposition reaction using the Nextera Tn5 Transposase (Nextera kit, Illumina #FC-121-1030). After 30 min at 37° C, the solution containing the nuclei was purified using the MinElute PCR Purification kit (Qiagen, #28004) and the transposed DNA was eluted in 10µl of Elution buffer and stored in -20° C, if not immediately used. Barcoded adapters (6) were added to the transposed fragments by PCR with the NEBNext® High Fidelity 2x PCR Master Mix (NEB #M0541). To avoid saturation in our PCR, we initially performed 5 cycles and an aliquot (5 µl) was used to perform a qPCR in order to find the number of cycles needed and to avoid over-amplification. Nextera qPCR primers were used for the amplification. When the number was decided, the remaining 45 µl of the PCR reaction were amplified for the additional number of cycles. The total number was never more than 12. Finally, the samples were purified using the

AMPure XP beads (Agencourt, #A63881) and eluted in 20 μ l. Concentration was measured with Qbit and the quality of the samples was estimated from the using Bioanalyzer 2100 (Agilent). ATAC-seq samples were sequenced 50 or 75bp paired-end and each experiment was performed in duplicates.

3C-Library for Capture Hi-C and 4C-seq

3C-libraries were prepared from at least 10-12 pairs of homozygous E10.5 forelimb and hindlimb buds as described previously (7–9). In summary, nuclei pellets were thawed on ice and used for DpnII digestion, ligation and de-crosslinking. To check the 3C-library, 500 ng was loaded on a 1% gel together with the undigested and digested aliquots. Further processing steps for 3C libraries for Capture Hi-C and 4C-seq can be found in SI Appendix Methods

Capture Hi-C

Re-ligated products were then sheared using a Covaris sonicator (duty cycle: 10%, intensity: 5, cycles per burst: 200, time: 2 cycles of 60 s each, set mode: frequency sweeping, temperature: 4 to 7 °C). Adaptors were added to the sheared DNA and amplified according to Agilent instructions for Illumina sequencing. The library was hybridized to the custom-designed SureSelect beads and indexed for sequencing (50 or 75 bp paired-end) following Agilent instructions. The cHiC SureSelect library was designed over the genomic interval (mm9, chr5:27800001-30600000) using the SureDesign tool from Agilent. Capture Hi-C experiments were performed in two technical replicates. However, CHi-C from wildtype limbs was performed in two biological replicates, one biological replicate divided in two technical and merged together for the generation of the final map. As an internal control, we compared the results from six experiments for regions outside of the region of interest (chr16:91,000,000-91,550,000 and chr17:26,340,001-27,200,000).

4C-seq

The 4C-seq libraries were performed as described previously (8, 9). In summary, 4-bp cutters (DpnII and Csp6I) were used as primary and secondary restriction enzymes. For each viewpoint, a total of 1 to 1.6 μ g DNA was amplified by PCR with the following primers associated with the respective restriction enzymes: Shh_read primer: 5'-CTACACGACGCTCTTCCGATCTCCATCGCAGCCCCAGTCT-3', Shh_reverse primer: 5'-CAGACGTGTGCTCTTCCGATCTCCATCCCCAGATGTGAGTGT-3'. All samples were sequenced 100 bp paired-end with Illumina Hi-Seq technology according to standard protocols. 4C-seq experiments from all viewpoints were carried out in duplicates.

3D polymer modeling

Simulation details. We modelled the genomic region chr5:27,800,001-30,600,000 (mm9) encompassing the mouse *Shh* gene, in the limb wildtype and *ACTCF i4:i5* cases. Based on our limb cHi-C interaction data (10kb resolution) our machine learning procedure (2) returns a polymer model with 12 different types of binding sites for each case (Figure S2A-B). A comparison between the experimental and the model obtained equilibrium contact matrices (Figure S2A-B) shows that the model well recapitulates the experimental contacts pattern, as also illustrated by the comparatively high values of the Pearson's correlation coefficient (r) that equals to 0.97 in both cases. To better measure the similarity between the matrices, accounting for the effects of the genomic proximity, we also computed the distance-corrected Pearson's correlation coefficient, r' , where we subtracted from the matrices the average contact frequency at each genomic distance before computing the correlation. The values of r' are 0.87 in the limb wildtype and 0.86 in *ACTCF i4:i5* model.

In order to obtain an ensemble of 3D 'single-molecule' conformations of the studied loci, we employed a polymer chain of $N=3,360$ beads and ran MD simulations starting from initial self-avoiding walk configurations (at least 10^2 independent simulations in each case). Then, we let the polymer evolve up to 10^8 time steps to reach stationarity, using interaction potentials derived

from classical studies of polymer physics (3). MD simulations were run using the LAMMPS software (4), with a simulation box at least two times larger than the gyration radius of the self-avoiding walk polymers to minimize finite-size effects. All details about the PRISM method and MD simulations are described in (2, 5). Figure 4D shows a representative 3D structure of the *Shh* locus in the limb wildtype (left) and $\Delta CTCF\ i4:i5$ (right) cases, as resulting from the modeling. To better compare the spatial location of *Shh* and its regulatory elements in the two different studied cases, a coarse-grained version of the simulated polymer is used. The beads coordinates were interpolated with a smooth third-order polynomial spline curve and the figures were produced using POV-Ray 3.7.0 (Persistence of Vision Raytracer Pty. Ltd).

Finally, we investigated the physical distances among the regions of interest (Figure 4E and Figure S2C). More precisely, Figure S3C shows the changes in relative distance among *Shh* and its regulatory regions, computed as $(d_{WT} - d_{i4:i5})/d_{WT}$, d_{WT} and $d_{i4:i5}$ being the average distances among the highlighted region in limb wildtype and $\Delta CTCF\ i4:i5$, respectively. The distribution of distances between *Shh* and its enhancer *ZRS* (Figure 4E), normalized by their average distance in the limb wild type, is statistically different in the limb wildtype (red) and $\Delta CTCF\ i4:i5$ (blue) cases (p-value $< 10^{-3}$, Mann-Whitney test).

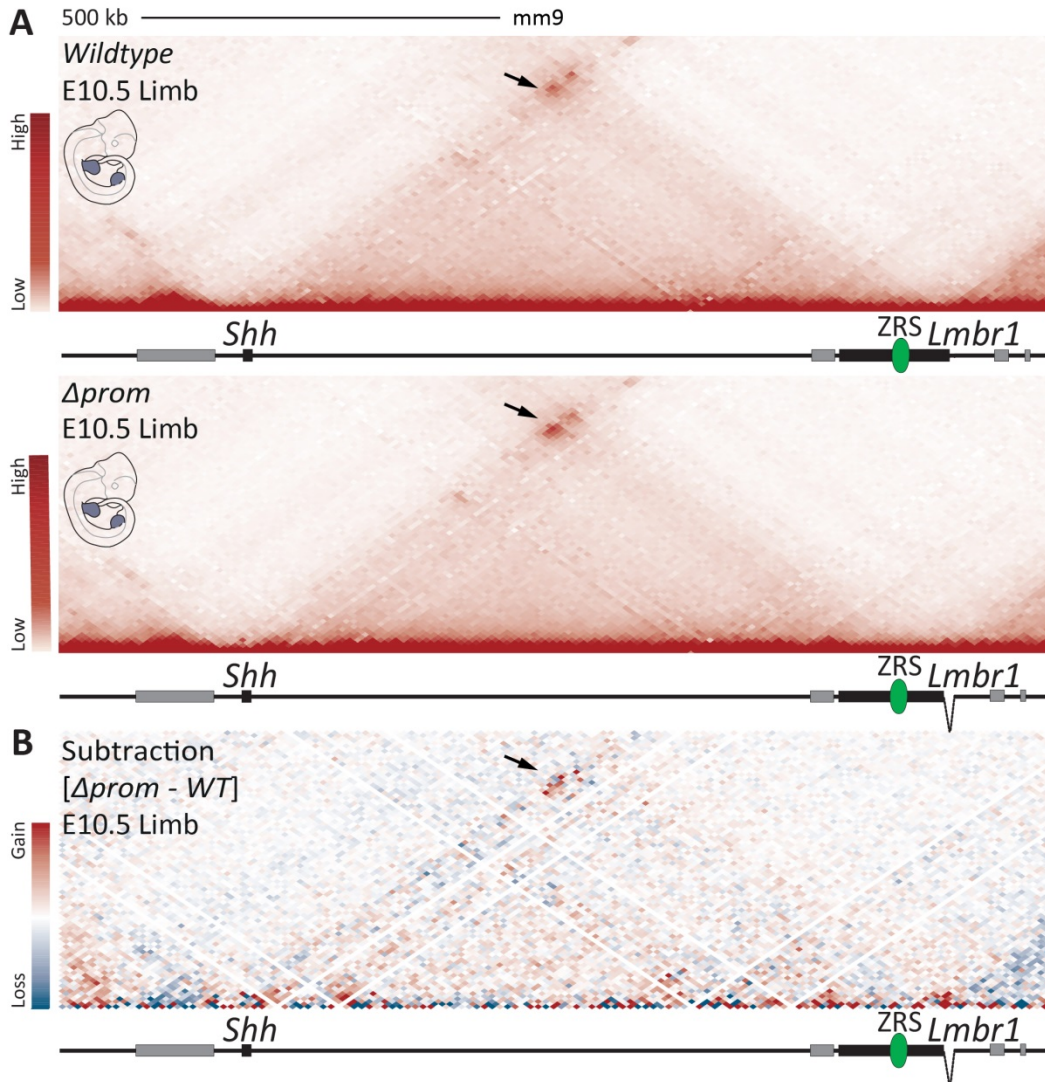


Fig. S1. Loss of transcription causes slight shift of interactions

A. cHi-C maps of wildtype and *Lmbr1*^{Δprom/Δprom} E10.5 limb buds. The black arrows indicate the differential interaction of the *Shh*-ZRS region between wildtype and *Lmbr1*^{Δprom/Δprom} E10.5 mutants. Note that the overall structure does not change between the wildtype and mutant limb buds. **B.** Subtraction map between wildtype and *Lmbr1*^{Δprom/Δprom} maps, where red and blue indicate gain and loss of contact, respectively, in *Lmbr1*^{Δprom/Δprom} mutant limbs. The black arrow indicates the increase of interaction between *Shh* and the centromeric part of the *Lmbr1* gene in *Lmbr1*^{Δprom/Δprom} mutants.

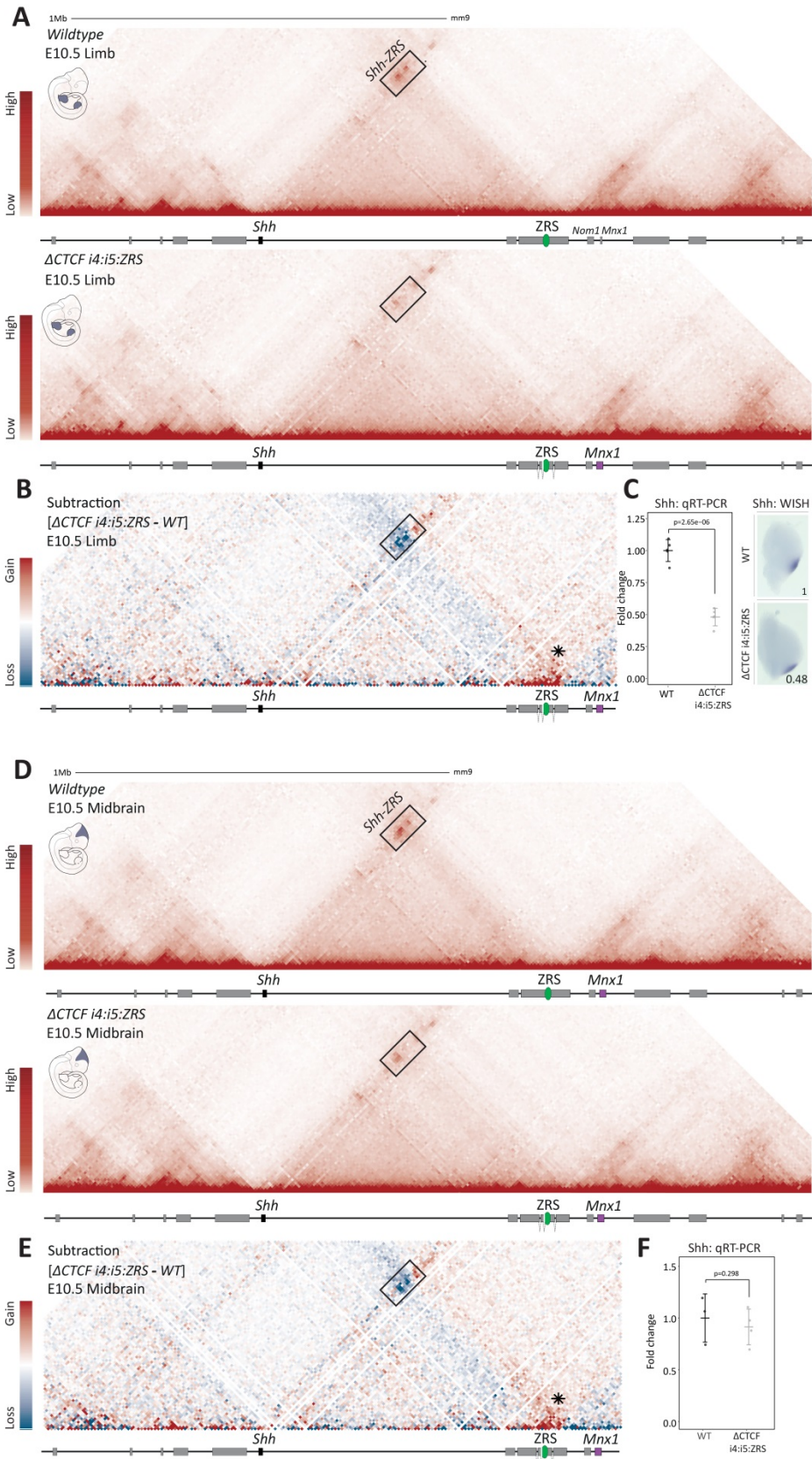


Fig. S2. CTCF sets the long-range interaction between *Shh* and ZRS

A. Limb wildtype (upper) and Δ CTCF *i4:i5:ZRS* (lower) ChIP maps. The black box indicates the domain of high interaction between *Shh* and the telomeric side of *Lmbr1*, which comprises the ZRS enhancer. Note the decreased interaction within the box in Δ CTCF *i4:i5:ZRS* compared to wildtype tissue. **B.** Subtraction map between wildtype and Δ CTCF *i4:i5* limb maps, where red and blue indicate gain and loss of contact, respectively, in mutants. The black asterisk indicates the loss of insulation between *Shh* and *Mnx1* TADs. **C.** qRT-PCR and WISH of *Shh* in wildtype (n=5) and Δ CTCF *i4:i5:ZRS* (n=5) limb buds. The p-value was calculated using a one sided Student t-test. Error bars represent standard deviation (SD). **D.** Midbrain wildtype (upper) and Δ CTCF *i4:i5:ZRS* (lower) ChIP maps. The black box indicates the domain of high interaction between *Shh* and the telomeric side of *Lmbr1*, which comprises the ZRS enhancer. Note the decreased interaction within the box in Δ CTCF *i4:i5:ZRS* compared to wildtype tissue. **E.** Subtraction map between wildtype and Δ CTCF *i4:i5* midbrain maps, where red and blue indicate gain and loss of contact, respectively, in mutants. The black asterisk indicates the loss of insulation between *Shh* and *Mnx1* TADs. **F.** qRT-PCR of *Shh* in wildtype (n=3) and Δ CTCF *i4:i5:ZRS* (n=2 biological, divided in 2 technical replicates each) limb buds. The p-value was calculated using a one sided Student t-test. Error bars represent standard deviation (SD).

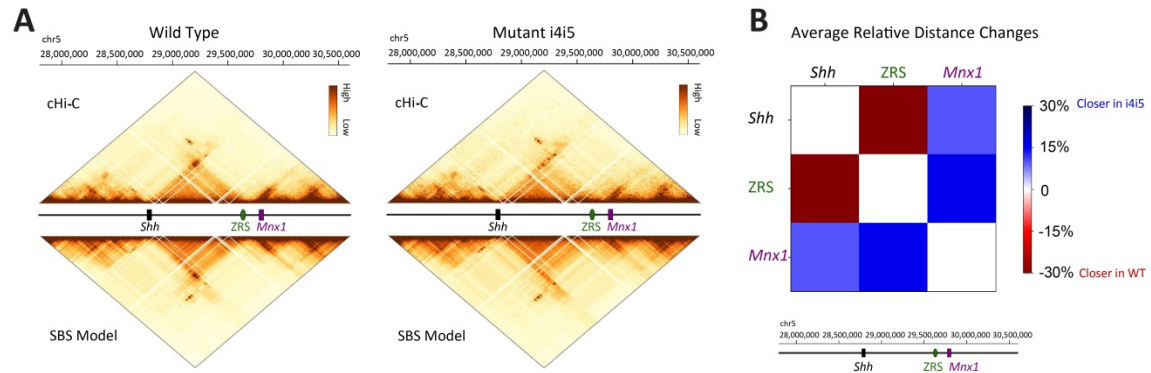


Fig. S3. *Shh* locus 3D modeling and physical distances.

A. (Top) Contact maps from cHi-C (above) and SBS model (below) in the limb wildtype have a Pearson correlation, r , and the distance-corrected Pearson correlation, r' , respectively equal to $r = 0.97$, $r' = 0.87$. (Bottom) . **B.** (Top) Contact maps from cHi-C (above) and SBS model (below) in the limb $\Delta CTCF$ *i4:i5* have a Pearson correlation, r , and the distance-corrected Pearson correlation, r' , respectively equal to $r = 0.97$, $r' = 0.86$. (Bottom). **C.** Relative distance changes between the limb wildtype and $\Delta CTCF$ *i4:i5*, averaged over the single-molecule population from the polymer modeling (see Methods).

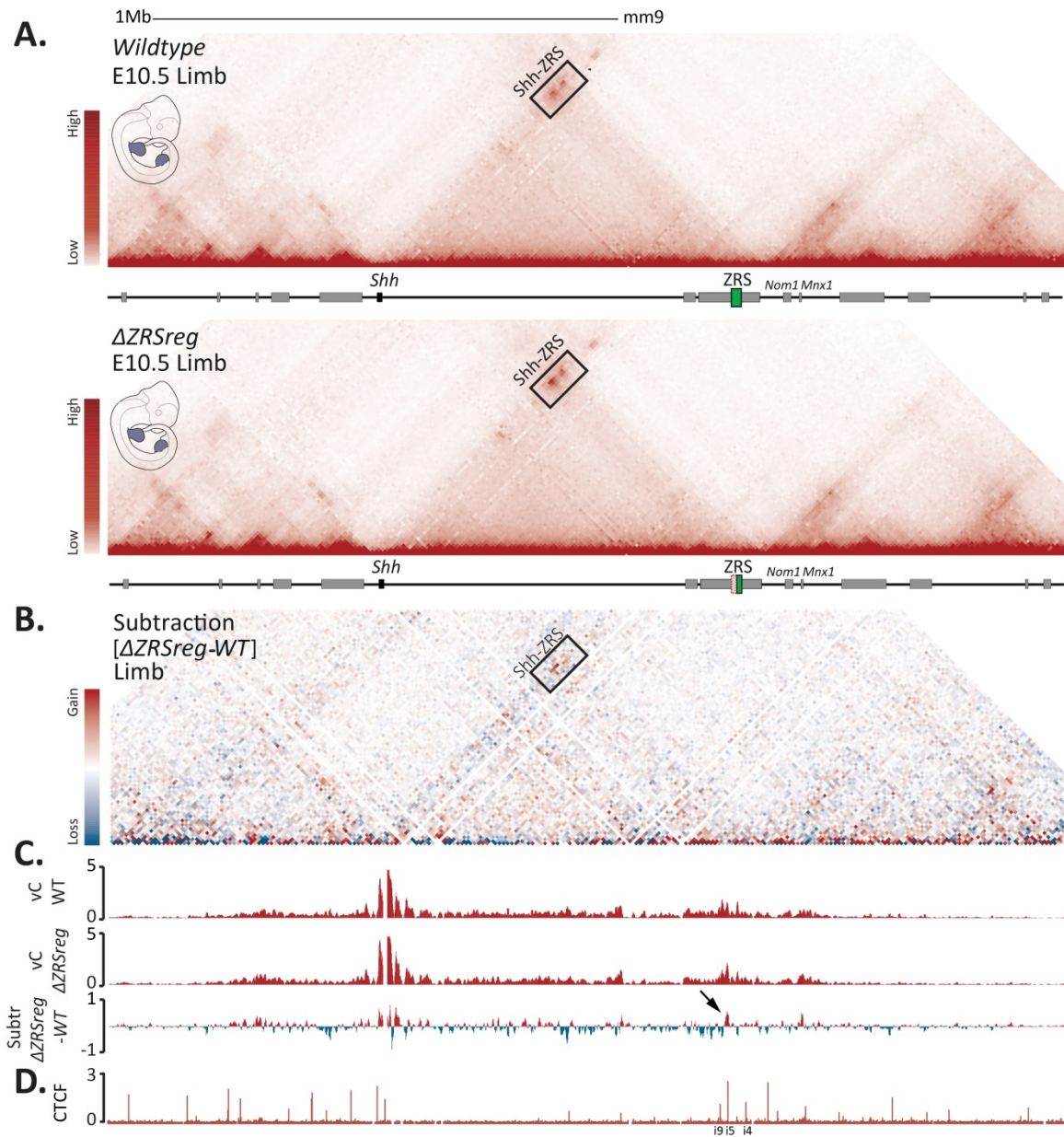


Fig. S4. The hypomorphic ZRS mutation does not modify the overall Shh TAD architecture.

A. Limb wildtype (upper) and $\Delta ZRSreg$ (lower) ChI-C maps. The black box indicates the domain of high interaction between *Shh* and the telomeric side of *Lmbr1*, which comprises the ZRS enhancer. Note the decreased interaction within the box in $\Delta ZRSreg$ compared to wildtype tissue. **B.** Subtraction map between wildtype and $\Delta ZRSreg$ maps, where red and blue indicate gain and loss of contact, respectively, in the mutant limbs. **C.** Virtual capture-C (vC) from the *Shh* promoter as viewpoint in wildtype and $\Delta ZRSreg$ limb buds. Subtraction track between mutants and wildtype shows gain (red) or loss (blue) of interaction in the mutant. Note the slight increase of interaction with the CTCF i5 (black arrow), shown by **(D)** ChIP-seq in wildtype limbs.

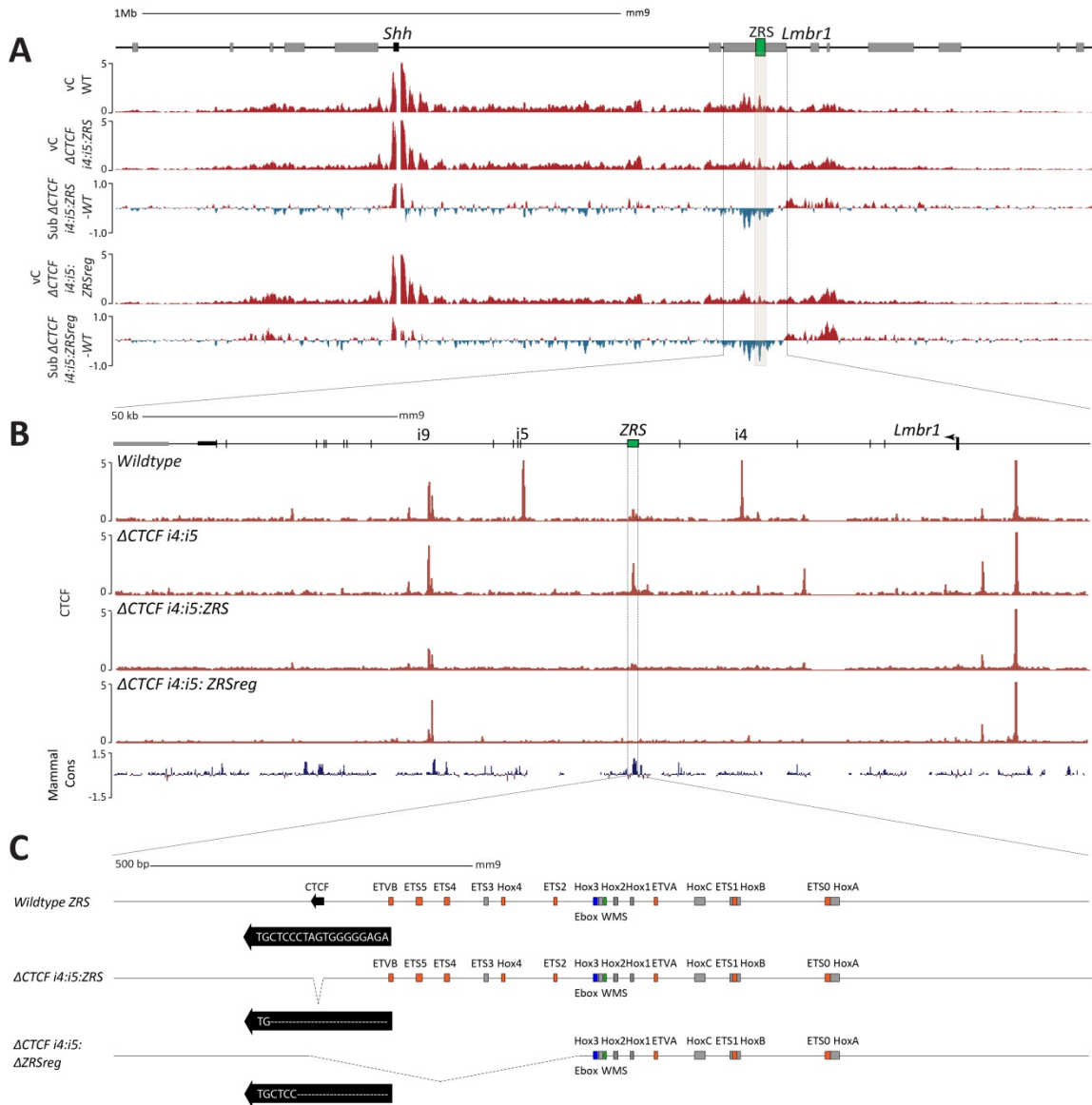


Figure S5: Comparison of Δ CTCF *i4:i5:ZRS* and Δ CTCF *i4:i5:ZRSreg* structure and genomic sequence

A. Virtual capture-C (vC) with the *Shh* promoter as viewpoint in wildtype, Δ CTCF *i4:i5:ZRS* and Δ CTCF *i4:i5:ZRSreg* limb buds. Subtraction tracks between mutants and wildtype are presented below each mutant vC track, where red indicates gain and blue indicates loss of interaction in the mutant. Both subtraction tracks show decrease of interaction with the CTCF sites within the *Lmbr1* gene and the ZRS. Note that the interaction frequency with the ZRS enhancer is similar in both mutants (grey box). **B.** CTCF ChIP-seq tracks of wildtype, Δ CTCF *i4:i5*, Δ CTCF *i4:i5:ZRS* and Δ CTCF *i4:i5:ZRSreg* limb buds. Note that ZRS CTCF binding is absent in both Δ CTCF *i4:i5:ZRS* and Δ CTCF *i4:i5:ZRSreg* mutants. **C.** Zoom-in at the ZRS genomic sequence. Known transcription factor binding sites are depicted according to the literature terminology (10–14). ZRS CTCF site sequence is shown in wildtype, Δ CTCF *i4:i5:ZRS* and Δ CTCF *i4:i5:ZRSreg* alleles. The black arrow signifies the orientation of the ZRS CTCF site.

Genotype		Genomic sequence at i5 CTCF (chr5:29619921-29619969)	Genomic sequence at ZRS CTCF (chr5:29641336-29641385)	Genomic sequence at i4 CTCF (chr5:29662545-29662612)
Wildtype		CCTAGCAGCCTCTGG AGTCCT CTAGTGG CCAA CTGGAGAACTGCTTGCG	TCTGGAAAGAAACCAG TGCTCC TAGTGGGG GAG AGCAGAGAGTTCTGAT	AATTACTGGCTCACCATAGAGTTATCTTCTACT GCCAC TGCTGGTATC ACAAA TAGTTCAA AATAC
<i>ΔCTCF i4</i>	Mut 1	Wildtype	Wildtype	AATTACTGGCTCACCATAGAGTTATCTTCTACT GCCA -----AAAATAGTTCAA AATAC
	Mut 2			AATTACTGGCTCACCATAGAGTTA----- CACAAA TAGTTCAA AATAC
<i>ΔCTCF i5</i>	Mut 1	CCTAGCAGCCTCTGG AGTCCT -----CTGGAGAACTGCTTGCG	Wildtype	Wildtype
	Mut 2	CCTAGCAGCCT-----CTGCTTGCG		
<i>ΔCTCF i4:i5</i>	Mut 1	CCTAGCAGCCTCTGG AGTCCT -----CTGGAGAACTGCTTGCG	Wildtype	AATTA-----C
	Mut 2	CCTAGCAGCCT-----CTGCTTGCG		AATTACTGGCTCACCATAGAGTTA-----AAAATAGTTCAA AATAC
<i>ΔCTCF i4:i5:ZRS</i>	Mut 1	CCTAGCAGCCTCTGG AGTCCT -----CTGGAGAACTGCTTGCG	TCTGGAAAGAA----- AGAG CAGAGAGTTCTGAT	AATTA-----C
	Mut 2	CCTAGCAGCCT-----CTGCTTGCG	TCTGGAAAGAA ACCAGT -----CAGAGAGTTCTGAT	AATTACTGGCTCACCATAGAGTTA-----AAAATAGTTCAA AATAC

Table S1. CTCF binding sites and motif deletions

Coordinates of the CTCF sites i5, ZRS and i4. Genomic sequences of these regions are shown for wildtype and each mutant. The CTCF motifs are in bold. Each mutant bears a different mutation of the CTCF site on each allele.

Experiment	sgRNA sequence (5'→3')
<i>Lmbr1</i> ^{Δprom/Δprom} right breakpoint	TTTCCTGGACAACCGCGTTC
<i>Lmbr1</i> ^{Δprom/Δprom} left breakpoint	GAGTGTAGACAAGTCTTTCGT
ΔCTCF <i>i4</i> CTCF motif	tattttgtgataccagcagg
ΔCTCF <i>i5</i> CTCF motif	ggagtcctctagtgccaac
ΔCTCF <i>i4:i5:ZRS</i> ZRS CTCF motif	GAAACCAGTGCTCCCTAGTG
ΔZRS <i>Reg</i> left breakpoint	GAAACCAGTGCTCCCTAGTG
ΔZRS <i>Reg</i> right breakpoint	CTGAGACAAATTAGCCACTG

Table S2. sgRNAs for CRISPR/Cas9 targeting

Guide RNAs used for all CRISPR/Cas9 genetic mutations of this study. For the CTCF motif targeting, one sgRNA was used. To induce larger mutations, two sgRNAs were used: one centromeric and one telomeric to the targeted sequence.

Movie S1. SBS-based modeling of the *Shh* locus from *Wildtype* cHiC maps

3D polymer model of wildtype limb cHi-C data. Note that the *Shh* gene (black) and the *ZRS* enhancer (green) are in close proximity and separated from the *Mnx1* (purple) gene.

Movie S2. SBS-based modeling of the *Shh* locus from Δ CTCF *i4:i5* cHiC maps

3D polymer model of mutant Δ CTCF *i4:i5* limb cHi-C data. In comparison with the Movie S1, note the reduced proximity between *Shh* (black) and the *ZRS* (green), but also the increased proximity between *Shh* and *Mnx1* (purple).

References

1. Andrey G, Spielmann M (2017) CRISPR/Cas9 Genome Editing in Embryonic Stem Cells. *Enhancer RNAs: Methods and Protocols, Methods in Molecular Biology*, ed Ørom UA (Springer New York, New York, NY), pp 221–234.
2. Bianco S, et al. (2018) Polymer physics predicts the effects of structural variants on chromatin architecture. *Nat Genet* 50(5):662–667.
3. Kremer K, Grest GS (1990) Dynamics of entangled linear polymer melts: A molecular-dynamics simulation. *J Chem Phys* 92(8):5057–5086.
4. Plimpton S (1995) Fast parallel algorithms for short-range molecular dynamics. *J Comput Phys* 117(1):1–19.
5. Chiariello AM, Annunziatella C, Bianco S, Esposito A, Nicodemi M (2016) Polymer physics of chromosome large-scale 3D organisation. *Sci Rep* 6:29775.
6. Buenrostro JD, Giresi PG, Zaba LC, Chang HY, Greenleaf WJ (2013) Transposition of native chromatin for fast and sensitive epigenomic profiling of open chromatin, DNA-binding proteins and nucleosome position. *Nat Methods* 10(12):1213–8.
7. Kragesteen BK, et al. (2018) Dynamic 3D chromatin architecture contributes to enhancer specificity and limb morphogenesis. *Nat Genet* 50(10):1463–1473.
8. van de Werken HJG, et al. (2012) 4C Technology: Protocols and Data Analysis. *Methods Enzymol* 513:89–112.
9. Franke M, et al. (2016) Formation of new chromatin domains determines pathogenicity of genomic duplications. *Nature* 538(7624). doi:10.1038/nature19800.
10. Galli A, et al. (2010) Distinct roles of Hand2 in initiating polarity and posterior Shh expression during the onset of mouse limb bud development. *PLoS Genet* 6(4). doi:10.1371/journal.pgen.1000901.
11. Lettice LA, et al. (2012) Opposing functions of the ETS factor family define Shh spatial expression in limb buds and underlie polydactyly. *Dev Cell* 22(2):459–67.
12. Leal F, Cohn MJ (2016) Loss and Re-emergence of Legs in Snakes by Modular Evolution of Sonic hedgehog and HOXD Enhancers. *Curr Biol* 26(21):2966–2973.
13. Kvon EZ, et al. (2016) Progressive Loss of Function in a Limb Enhancer during Snake Evolution. *Cell* 167(3):633–642.e11.
14. Lettice LA, Devenney P, De Angelis C, Correspondence REH, Hill RE (2017) The Conserved Sonic Hedgehog Limb Enhancer Consists of Discrete Functional Elements that Regulate Precise Spatial Expression. *CellReports* 20(6):1396–1408.